

## Complex Quasiperiodic and Chaotic States Observed in Thermally Induced Oscillations of Gas Columns

T. Yazaki, S. Takashima, and F. Mizutani<sup>(a)</sup>

*Department of Physics, Aichi University of Education, Igaya-chō, Kariya-shi, 448, Japan*

(Received 30 September 1986)

Highly nonlinear phenomena are observed in Taconis oscillations, which are spontaneous oscillations of gas columns thermally induced in a tube with steep temperature gradients. Near the overlapped region and the intersection of the stability curves for two different modes with incommensurate frequencies, we find that both modes can be excited simultaneously and competition between them leads to complex quasiperiodic and chaotic states. Experimental data are analyzed by use of recent methods from the theory of nonlinear dynamical systems.

PACS numbers: 47.25.Ae, 05.45.+b, 05.70.Ln, 43.90.+v

Spontaneous acoustic oscillations of gas columns can be generated in a tube with steep temperature gradients without external mechanical force. Most experimenters in cryogenics often observe this type of oscillations when a tube closed at the top end is inserted into liquid helium, and call them "Taconis oscillations." This phenomenon is associated with thermally driven acoustic oscillations as well as the Sondhauss tube and the Rijke tube<sup>1</sup>; namely, some heat is converted to work under proper conditions and this leads to self-sustained acoustic oscillations.<sup>2</sup> In recent years thermoacoustics has received considerable interest in connection with related fields of application.<sup>3</sup> As fundamental studies, however, only the stability curves have been theoretically<sup>4</sup> and experimentally<sup>5</sup> determined in the small-amplitude limit. This paper is the first report on nonlinear phenomena observed in this new acoustic system, where competition between two different resonance modes simultaneously induced in large-amplitude regimes gives rise to complex quasiperiodic and chaotic states.

The experimental system is schematically shown in Fig. 1. A step-functional temperature distribution along the tube closed at both ends is symmetrically established by an external method. A gas column in the tube consists of three parts; homogeneous temperatures (warm,  $T_H$ , and cold,  $T_C$ ) and temperature-jump regions. The cavities used in these experiments were stainless-steel tubes of inner radii  $r = 1.2, 2.2,$  and  $3.7$  mm, wall thickness  $0.3$  mm, and whole tube lengths  $2.1$  and  $2.9$  m. The length  $\Delta X$  was less than  $4\%$  of  $L$ . The warm part was maintained at  $296$  K and temperatures at the cold part, stretched as U shaped at  $X=0$ , could be varied continuously from  $4.2$  to  $45$  K by the method of continuous flow of cold helium gas.<sup>5</sup> The time dependence of the pressure and the mean pressure were measured by two small pressure transducers attached at the two closed ends with excellent linearity over a wide range. The signal voltage  $V(t)$  was digitized by a fast twelve-bit analog-to-digital converter. Calculation of power spectra via the fast-Fourier-transform algorithm and plotting of trajectories in phase space were performed from  $8 \times 10^3$  or

$16 \times 10^3$  points sampled by suitable times.

The stability curve and the frequency ( $f_1$ ) for the lowest mode were given by Rott's theory<sup>4</sup> where the temperature had a discontinuity at  $X = \pm l$  and effects of both thermal conductivity and viscosity of the gas were taken into account. The important dimensionless numbers characterizing the boundary of the stability-instability in this system are given by

$$Y_C = r(\omega/a_C)^{1/2} \text{ and } Y_H = r(\omega/a_H)^{1/2}, \quad (1)$$

where  $Y$  is the ratio of the tube inner radius to thickness  $\delta \sim (a/\omega)^{1/2}$  of the thermal boundary layer formed on the tube wall ( $a$  is the thermal diffusivity of gas, and  $\omega$  is the angular frequency) and subscripts  $H$  and  $C$  show the warm and the cold, respectively. In experimental works<sup>5</sup> it was verified that the stability curves could be unified by Eq. (1) for the fundamental. In order to draw up the phase diagrams of the higher frequency modes in addition to the fundamental we adopt the following numbers independent of the frequency instead of Eq. (1):

$$R = Y_C \lambda^{-1/2} \text{ and } T_H/T_C = (Y_C/Y_H)^{2/(1+\beta)}, \quad (2)$$

where the dimensionless frequency  $\lambda$  is defined by  $\omega l/a_C$  ( $a_C$  is the adiabatic sound velocity at the cold part) and  $\beta$  is  $0.647$  for helium gas.

The experimental phase diagram is shown in Fig. 2, where the working gas is helium and the ratio between lengths of warm and cold parts,  $(L-l)/l$ , is  $0.3$ . The neutral points were explored by gradual variation of  $R$  through the mean density of the gas. When the temper-

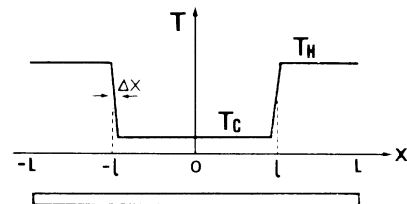


FIG. 1. Mean temperature distribution along the tube closed at both ends.

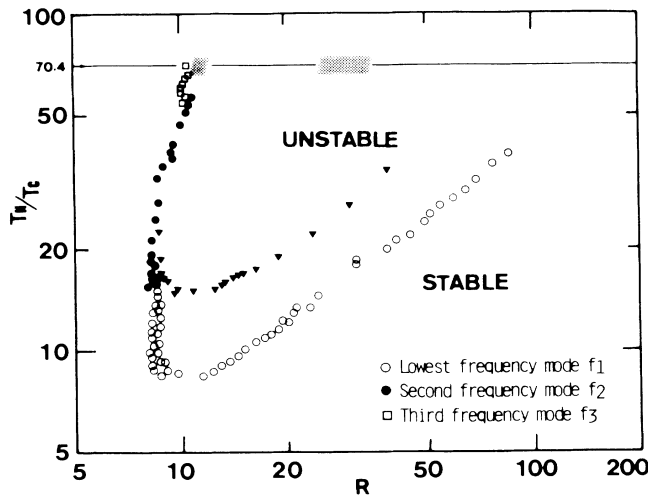


FIG. 2. Experimental phase diagram as a function of temperature ratio  $T_H/T_C$  vs  $R=r(ac/ac_l)^{1/2}$ . Under constant temperature ratio  $T_H/T_C=70.4$  competition between two adjacent oscillatory modes leads to quasiperiodic states in the shaded regions. Stability limits for an asymmetric tube closed at  $X=0$  and  $L$  are shown by solid triangles.

ature ratio exceeds some threshold value dependent on  $R$ , the gas column begins to oscillate with sinusoidal waveforms. There are two stability limits corresponding to the left- and right-hand branches, where the oscillating gas approaches isothermal and adiabatic reversible processes, respectively. The heat flux and the acoustic-energy source are absent in such reversible processes.<sup>6</sup> A

gas column needs a suitable thermal boundary-layer thickness (irreversible process) to maintain the oscillation. Therefore at the left-hand branch rapider motions (higher frequency modes) with thinner layers can be induced instead of the fundamental. The second ( $f_2$ ) and the third ( $f_3$ ) frequency modes, which have two and three pressure nodes at cold parts, respectively, appear at such a branch. Appearance of the second mode suggests that the oscillation can be induced in an asymmetric tube closed at  $X=0$ . We found the oscillation for such a tube, whose stability curve (solid triangles in Fig. 2) smoothly joins to that of the second mode. Moreover, the experimental curves agreed well with the theoretical curves derived from the key equations.<sup>4,7</sup>

The intersection of the stability curves of different modes with incommensurate frequencies allows us to expect interesting phenomena to occur in the interior of the curve where amplitudes surprisingly become large ( $\sim 10^4$  Pa). In the shaded regions in Fig. 2, two adjacent oscillatory modes are simultaneously excited and competition between them leads to complex quasiperiodic states. Experiments were performed at a constant temperature ratio (70.4); the warm and the cold parts were always immersed into a 296-K reservoir and liquid helium at 4.2 K, respectively.

The observed sequence of pressure records (a small portion of the duration of each record) and corresponding power spectra for gradual increasing control parameter  $R$  are shown in Fig. 3. A pure periodic motion of the third mode [Fig. 3(a)] is spontaneously generated at  $R=10.4$ . The value of  $\lambda$  is 4.14, which means that three

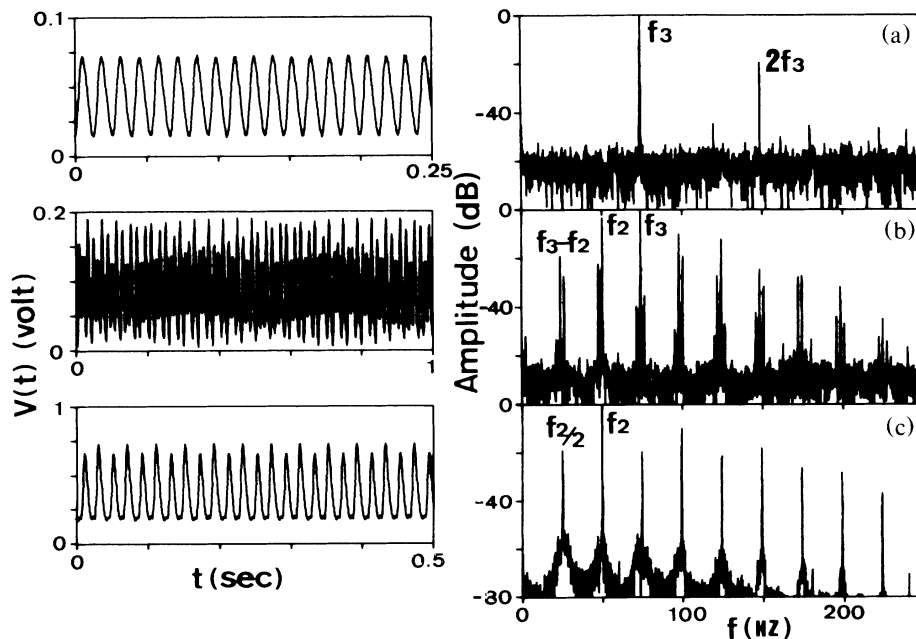


FIG. 3. Time records of the pressure ( $5.5 \times 10^3$  Pa/V) and corresponding power spectra. (a)  $R=10.8$ , a periodic state of the third frequency mode ( $f_3$ ); (b)  $R=11.7$ , a quasiperiodic state; (c)  $R=14.7$ , a period doubling.

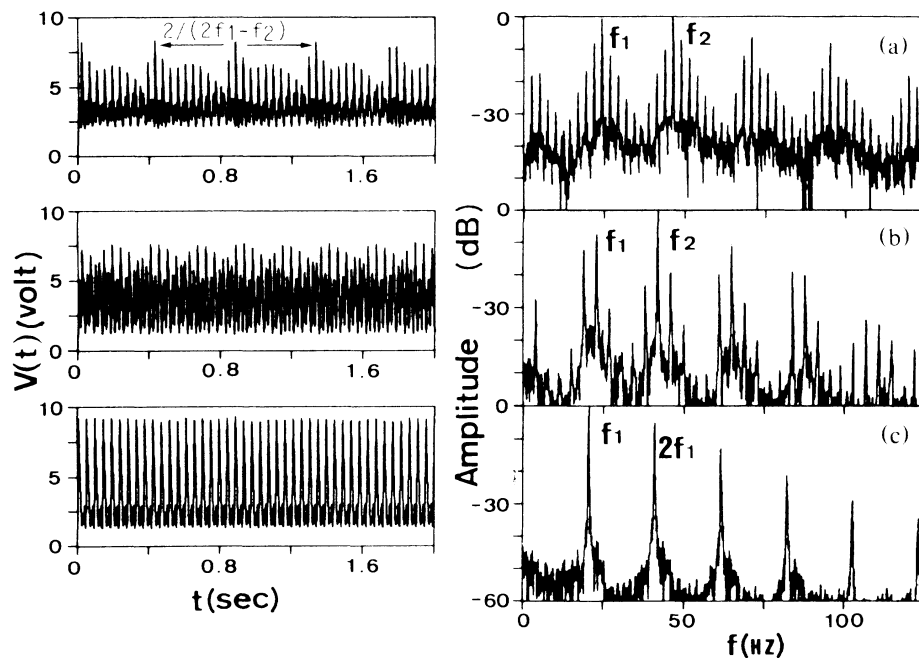


FIG. 4. Time records of the pressure ( $5.5 \times 10^3$  Pa/V) and corresponding power spectra. (a)  $R=25.2$ , cockscomb pattern with sharp peaks above the onset of noise; (b)  $R=32.2$ , a quasiperiodic state; (c)  $R=35.8$ , a periodic state of the fundamental ( $f_1$ ).

pressure nodes exist at the cold part. In a small region of  $R$  (the first shaded area in Fig. 2), the second frequency mode begins to grow, and both modes are simultaneously induced. Interaction between them leads to a quasiperiodic state [Fig. 3(b)] slowly modulated at low frequency where the spectrum consists of the sharp peaks of  $f_2$ ,  $f_3$ , and mixing components of their linear combination. Phase locking of two frequencies and chaotic behavior were not found in this region, where the variation of the frequency ratio  $f_2/f_3$  ( $=0.667$ ) is less than 0.3%. The quasiperiodic motion turns into the periodic state of  $f_2$  for further increase of control parameter. This sequence depends on the history of the system and exhibits hysteresis. A quasiperiodicity does not occur for gradual decreasing control parameter but the transition from the second mode of the third mode occurs at a position close to the extrapolated line of the stability curve of the second mode. A further increase of  $R$  results in one period doubling [Fig. 3(c)] but no cascade of period-doubling bifurcation occurs. The system returns to the periodic motion of  $f_2$  again.

In the process of the transition from the second mode to the fundamental, competition between them takes place in the second shaded region in Fig. 2. The typical examples of waveforms and power spectra are shown in Fig. 4. The amplitude modulated as "cockscomb" patterns, which are characterized by a sudden jump in amplitude, appears at  $R=25.2$  [Fig. 4(a)]. The spectrum shows the increase of a visible noise floor in addition to

higher-order mixing components due to strongly coupled nonlinear oscillations. Near the onset of chaos such cockscomb patterns have been also observed in the other acoustic system, Faraday experiment.<sup>8</sup> A further increase of  $R$  leads to smooth modulation and decrease of the number of the peak spectrum [Fig. 4(b)]. Mode competition disappears and the system is absorbed into the periodic motion of  $f_1$  near  $R=35$  [Fig. 4(c)]. The rotation number,  $f_1/f_2$ , increases gradually without a perceptible phase-locked state. The frequency parameters  $\lambda_1$  ( $=\omega_1 l/a_C$ ) and  $\lambda_2$  ( $=\omega_2 l/a_C$ ) asymptotically tend to  $\pi/2$  and  $\pi$ , respectively, as the system approaches the left-hand branch (Fig. 5). This behavior shows that as the viscous boundary-layer thickness becomes thicker in the warm part, the positions of the temperature jump act almost like those at the closed end.

We analyzed experimental data using the theory of nonlinear dynamical systems. Phase portraits of dimension  $m$  can be constructed from the vectors  $\{V(t_i), V(t_i + \tau), \dots, V(t_i + (m-1)\tau)\}$  for the digital time series  $V(t_i)$  of signal voltage, where the delay time  $\tau$  is an arbitrary fixed value.<sup>9</sup> Two-dimensional projections of three-dimensional phase portraits constructed by plotting of the voltages  $V(t_i)$ ,  $V(t_i + \tau)$ , and  $V(t_i + 2\tau)$  are presented in the upper row in Fig. 6, where  $\tau$  is chosen to be about  $\frac{1}{4}$  of the period of the intrinsic oscillation. The lower row in Fig. 6 shows Poincaré sections given by the intersection of trajectories in three-dimensional phase portraits with the plane passing through the dashed line

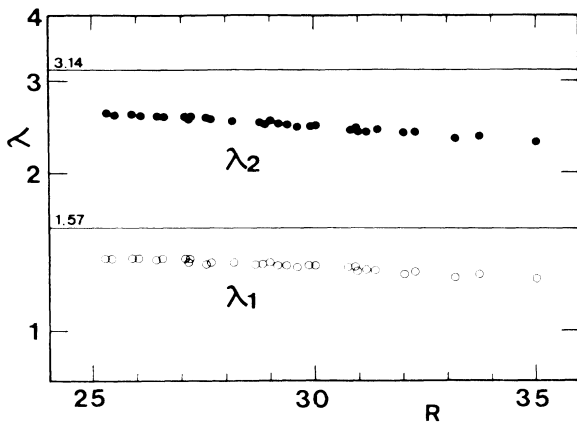


FIG. 5. Dimensionless frequency parameter  $\lambda (= \omega l / a_c)$  of two modes ( $f_1$  and  $f_2$ ) in the quasiperiodic regime.

in the upper part of Fig. 6. For the quasiperiodic state in Fig. 3(b) the trajectories in the phase space cover the whole torus, and the Poincaré section is a well-defined closed loop [Fig. 6(a)]. The phase portrait corresponding to the cockscomb pattern in Fig. 4(a) shows a state just at the onset of chaos [Fig. 6(b)]. Although the Poincaré section is still clear, wrinkles start appearing on the torus, which can be caused by increasing nonlinear interaction due to coupling between two oscillatory modes. Recently, using U tubes more smoothly connected at  $X=0$  we have observed chaotic motions developed from cockscomb patterns at smaller control parameters, where a torus is not apparent and the Poincaré section no longer yields useful information [Fig. 6(c)]. In order to document the deterministic chaos, using 8000 sampling points we calculated the correlation integrals  $C_m(\epsilon)$  introduced by Grassberger and Procaccia,<sup>10</sup> which show the possibility that two points at the attractor are separated by a distance smaller than  $\epsilon$  and scale as  $C_m(\epsilon) \sim \epsilon^\nu$ . The dimension of the attractor was determined from correlation exponent  $\nu$  which was plotted as a function of the embedding dimension  $m$  ( $=1, 2, \dots, 10$ ). We got good convergence of stationary values which are  $\nu = 2.18 \pm 0.03$  and  $2.87 \pm 0.06$  for the attractors of Figs. 6(b) and 6(c), respectively. The fractal asymptotic value of  $\nu$  indicates the existence of the strange attractor.

The transition to chaos has been observed in several acoustic systems<sup>11</sup> where the route to chaos is a sequence of a period-doubling bifurcations *à la* Feigenbaum. In particular the Faraday experiment by Ciliberto and Gollub<sup>12</sup> showed that the chaotic behavior arises from competition between different spatial modes or patterns. Theoretical works in parallel with the experiment were performed by Meron and Procaccia<sup>13</sup> in order to make clear the appearance of few-dimensional chaos in systems with an infinite number of degrees of freedom. Our experiments on chaos resemble the Faraday experiment

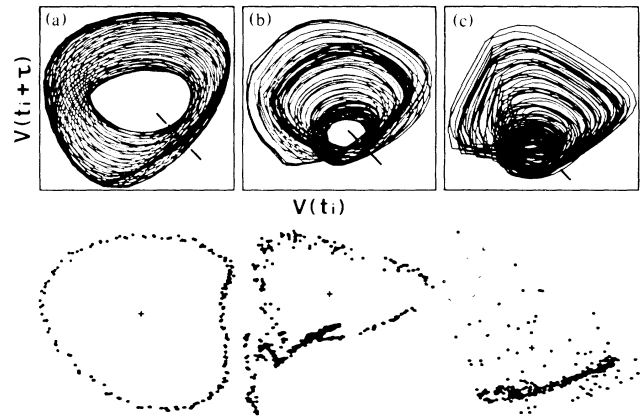


FIG. 6. Upper row, two-dimensional phase portraits; lower row, Poincaré sections. (a) and (b) correspond to Figs. 3(b) and 4(a), respectively, and (c) is a chaotic state at  $R=19.6$ .

in some respects; chaotic region and mechanism. However, there is no theoretical work to explain the bifurcation structure observed in Taconis oscillations.

This work was supported by a Grant in Aid for Scientific Research from the Ministry of Education (Grant No. 61740204). Thanks are due to the Institute for Molecular Science for the preparation of helium.

(a) Present address: National Institute for Physiological Sciences, 38 Nishigōnaka, Myōdaijichō, Okazaki 444, Japan.

<sup>1</sup>K. T. Feldman, Jr., *J. Sound Vib.* **7**, 71 (1968); K. Y. Feldman, Jr., *J. Sound Vib.* **7**, 83 (1968).

<sup>2</sup>J. W. Strutt, Baron Rayleigh, *Theory of Sound* (Dover, New York, 1945), sect. 3221i.

<sup>3</sup>J. Wheatly, T. Hofer, G. W. Swift, and A. Migliori, *J. Acoust. Soc. Am.* **74**, 153 (1985); J. Wheatly and A. Cox, *Phys. Today* **38**, No. 8, 50 (1985).

<sup>4</sup>N. Rott, *Z. Angew. Math. Phys.* **20**, 230 (1969), and **24**, 54 (1973).

<sup>5</sup>T. Yazaki, A. Tominaga, and Y. Narahara, *J. Low Temp. Phys.* **41**, 45 (1980).

<sup>6</sup>A. Tominaga, Y. Narahara, and T. Yazaki, *J. Low Temp. Phys.* **54**, 233 (1984).

<sup>7</sup>T. Yazaki, A. Tominaga, and Y. Narahara, *Phys. Lett.* **79A**, 407 (1980).

<sup>8</sup>R. Keolian, L. A. Turkevich, S. J. Putterman, and I. Rudnick, *Phys. Rev. Lett.* **47**, 1133 (1981).

<sup>9</sup>N. H. Packard, J. P. Crutchfield, J. D. Farmer, and R. S. Shaw, *Phys. Rev. Lett.* **45**, 712 (1980).

<sup>10</sup>P. Grassberger and I. Procaccia, *Phys. Rev. Lett.* **50**, 346 (1983), and *Physica (Amsterdam)* **9D**, 189 (1983).

<sup>11</sup>W. Lauterborn and E. Cramer, *Phys. Rev. Lett.* **47**, 1445 (1981); W. Lauterborn and E. Suchla, *Phys. Rev. Lett.* **53**, 2304 (1984); C. W. Smith, M. J. Tejwani, and D. A. Farris, *Phys. Rev. Lett.* **15**, 492 (1982).

<sup>12</sup>S. Ciliberto and J. P. Gollub, *Phys. Rev. Lett.* **52**, 922 (1984), and *J. Fluid Mech.* **158**, 381 (1985).

<sup>13</sup>E. Meron and I. Procaccia, *Phys. Rev. Lett.* **56**, 1323 (1986).